

Yale University

EliScholar – A Digital Platform for Scholarly Publishing at Yale

Yale Medicine Thesis Digital Library

School of Medicine

January 2021

Regulated Apoptosis In C. Elegans Development

Nathan Lifton

Follow this and additional works at: <https://elischolar.library.yale.edu/ymtdl>

Recommended Citation

Lifton, Nathan, "Regulated Apoptosis In C. Elegans Development" (2021). *Yale Medicine Thesis Digital Library*. 4012.

<https://elischolar.library.yale.edu/ymtdl/4012>

This Open Access Thesis is brought to you for free and open access by the School of Medicine at EliScholar – A Digital Platform for Scholarly Publishing at Yale. It has been accepted for inclusion in Yale Medicine Thesis Digital Library by an authorized administrator of EliScholar – A Digital Platform for Scholarly Publishing at Yale. For more information, please contact elischolar@yale.edu.

Regulated apoptosis in *C. elegans* development

A Thesis Submitted to the
Yale University School of Medicine
in Partial Fulfillment of the Requirements for the
Degree of Doctor of Medicine

by

Nathan Lifton

2021

Abstract

REGULATED APOPTOSIS IN CAENORHABDITIS ELEGANS DEVELOPMENT.

Nathan Lifton, Alison Kochersberger, and Marc Hammarlund, Department of Genetics, Yale University School of Medicine, New Haven, CT.

We have used chromosome engineering in *C. elegans* to develop a model animal in which cells normally undergoing developmental programmed cell death (DPCD) survive and are visibly marked. This system uses three elements: The first is a mutation in the apoptosis activator, *ced-3*, that drives developmental programmed cell death, such that cells normally killed by DPCD survive. The second is a cassette in which the gene encoding the bacterial enzyme Cre recombinase is expressed under transcriptional control of the regulatory elements of the *egl-1* gene (Cre protein induces homologous recombination between specific DNA sequence elements called LoxP elements). The third element is a green fluorescent protein (GFP) reporter gene that is connected to a constitutively active promoter; however, GFP cannot be produced from this construct without the expression of Cre because two exons of GFP are inverted within the gene and flanked by inverted LoxP sites. When Cre recombinase is expressed, it will induce flipping of exons 2 and 3 of GFP, resulting in an intact GFP that is constitutively expressed, providing a permanent mark for cells in which expression at the *egl-1* locus was activated even transiently.

We succeeded in producing worms with the desired constructs by injecting gonads with linear extrachromosomal arrays that were integrated at random sites in the genome by induction of double strand DNA breaks with trimethylpsoralen and ultraviolet light.

We developed multiple strains with independent insertions of the *egl-1/Cre* (4 independent insertions) and Cre-dependent GFP (3 independent insertions) cassettes, demonstrated that each had integrated into a single *C. elegans* chromosome, and performed crosses to produce worms that were homozygous at all three loci (*ced-3*, *egl-1/Cre* and Cre-dependent GFP).

Preliminary analysis of the resulting worms from two of these strains provides evidence of Cre-dependent GFP expression, with reproducible expression of GFP in cells of the posterior bulb of the pharynx, which includes the head ganglia.

Acknowledgements

First and foremost, I would like to thank everyone working in the Hammarlund lab for providing a warm working environment and a helping hand whenever needed, and for introducing me to the exciting world of *C. elegans*. In particular, I would like to thank Alison Kochersberger, PhD candidate, and my advisor and primary investigator Marc Hammarlund, PhD, who shepherded me through every stage of this project, and without whose collective brilliance and hard work this project would not exist. Thank you, also, to Curt Scharfe, PhD, for reviewing this thesis for the Department of Genetics.

I would also like to thank the Yale Office of Student Research for facilitating this research experience, and the NIH, which provided funding through an NCATS CTSA-TL1 Medical Student Research Fellowship.

Finally, I would like to thank my parents and Elizabeth, whose unconditional love and support has not only brought joy to my life, but has also made this thesis and all other achievements possible.

Research reported in this publication was supported by the National Center for Advancing Translational Sciences of the National Institutes of Health under Award Number TL1TR000141. The content is solely the responsibility of the authors and does not necessarily represent the official views of the National Institutes of Health.

Table of Contents

Introduction & Statement of Purpose.....	1
Methods.....	8
Results.....	16
Discussion.....	33
Figures.....	44
Tables.....	52
References.....	56

Introduction & Statement of Purpose

Developmental programmed cell death.

Developmental programmed cell death (DPCD), in which normal, healthy cells undergo apoptosis, is an extremely important process that occurs during the development of multicellular organisms. DPCD is essential for morphogenesis, sexual differentiation, and development of the immune and nervous systems¹⁻⁷.

DPCD can be divided into three phases: specification, killing, and execution. In the specification phase, individual cells receive signals that they are selected for death. In the killing phase, the apoptotic pathway is activated in these individual cells, the end point of which is initiation of the execution phase. In the execution phase, enzymes are induced that produce fragmentation and degradation of nuclear DNA⁸⁻¹⁴.

The cellular mechanisms that mediate the killing and execution phases are relatively well understood from elegant genetic studies in *C. elegans*. The killing phase is mediated by a pathway involving the genes *egl-1*, *ced-9*, *ced-4*, and *ced-3*. *ced-3* is a pro-apoptotic gene. The enzymatic activity of its encoded protein, a cysteine-aspartic acid protease (caspase), is sufficient for inducing the downstream execution phase, but needs to be activated by *ced-4*. *ced-4*, in turn is normally inhibited by *ced-9*, which in turn is inhibited by *egl-1*. Thus, in the absence of *egl-1*, the pathway is silent. But upon expression of *egl-1*, *ced-9* can no longer inhibit *ced-4*, which then activates *ced-3*, thereby activating the cell death pathway (Figure 1)^{3,15,16}. Expression of *egl-1* is normally the rate-limiting step in this process.

Downstream of *ced-3* are many genes whose functions perform the execution phase of cell death, including digestion of nuclear DNA and induction of phagocytosis by surrounding cells. Genes whose encoded proteins are involved in genome degradation include *nuc-1*, *cps-6*, *wah-1*, *crn-1*, 2, 3, 4, 5 and 6¹⁷⁻²⁰. Genes in the surrounding cells have been identified that are required for them to phagocytose the dying cells. These include *ced-1*, *ced-2*, *ced-5*, *ced-6*, *ced-7*, *ced-10*, *ced-12*, and *psr-1*²¹⁻²⁶. *ced-7* is translocated to the cell surface of the dying cell, promoting the cell's phagocytosis by surrounding cells.

The basic pathway of the killing phase has proved to be highly conserved across metazoans, which has contributed to biochemical understanding of the function of each gene's encoded protein²⁷. CED-3 in worms is homologous to mammalian caspases, proteases that are the executioners of cell death. CED-3 is at the top of a proteolytic cascade, activating downstream targets that ultimately activate single and double-stranded endonucleases and exonucleases, mediating nuclear genome degradation, as well as translocation of CED-7 to the cell surface. CED-4 is related to mammalian APAFs, which are proteins that are required for binding and activation of CED-3's caspase activity. *ced-9* encodes a protein homologous to BCL-2 proteins, which inhibit APAFs by directly binding to them and preventing their activation of CED-3-like caspases. *egl-1* is homologous to BH3 genes, which bind to and inhibit activity of BCL-2 proteins.

Similarly, many of the gene products involved in the engulfing cells' phagocytic activity have conserved functions across species. *ced-2*, *ced-5*, *ced-10*, and *ced-12* encode conserved components of the Rac GTPase signaling

pathway involved in regulating actin cytoskeleton rearrangement essential for cell migration and corpse engulfment. CED-2 is a CrkII-like adaptor with one SH2 and two SH3 (SRC Homology) domains²⁸. CED-5 is an analogue of the human DOCK180, which physically interacts with human CrkII.²⁹ CED-10 is a *C. elegans* homologue of mammalian Rac GTPase, which controls cytoskeletal dynamics and cell shape changes²⁸. Ced-12 contains a potential PH (pleckstrin-homology) domain and an SH3-binding motif^{23,25,26}.

Because programmed cell death kills normal cells, its regulation must be exquisitely precise. Tracing the lineage of every cell in *C. elegans* development demonstrates that the development of hermaphrodites is invariant, and that, of the 1090 cells generated during development of the soma, 131 specific cells always die via DPCD at specific stages—113 of these cells die during embryonic and 18 during post-embryonic development³⁰. Nonetheless, our understanding of the specification phase—the process by which these 131 individual cells are invariably selected to die—is incomplete.

In mammals, two alternative pathways can activate apoptosis. One is cell-autonomous (intrinsic), while the other is non-cell-autonomous (extrinsic). The intrinsic pathway is activated by loss of integrity of the mitochondrial membrane, releasing cytochrome C, which activates APAFs (homologs of CED-4). In *C. elegans*, it appears that cell death occurs by a pathway analogous to the intrinsic pathway. CED-9 holds CED-4 in an inactive form on the mitochondrial membrane, and EGL-1 binding to CED-9 releases CED-4, which can then activate CED-3.

The current model for cell death specification in *C. elegans* is that in the 959 cells destined to survive, *egl-1* expression is low or absent and that in the 131 cells destined to die, *egl-1* expression is at least transiently high, sufficient to induce the cell death pathway³¹. Thus, expression of *egl-1* is believed to be the rate-limiting step in initiation of DPCD.

Little is known about the regulators of *egl-1* expression. Cis-acting regulatory elements have been identified over a large region surrounding *egl-1*, both upstream and downstream of the gene, but only a handful of specific transcriptional regulators of *egl-1* have been identified. The first of these, the transcriptional inhibitor TRA-1, was discovered because of a mutation in the 3' regulatory region of *egl-1* that caused ectopic expression of *egl-1* due to loss of the TRA-1 binding site.

egl-1 was discovered by a gain of function mutation that causes *egl-1* to be expressed abnormally in neurons required for egg laying, producing an egg-laying defective (Egl) phenotype^{15,32}. This mutation results in defective egg laying due to death of neurons required for this activity. Screens for suppressors of the egg laying defect identified a loss of function allele in *egl-1* that prevented DPCD of virtually all of the 131 normally affected cells^{15,33}. Besides *tra-1*, transcription regulators that regulate *egl-1* have been identified for only 8 of the 131 cells that normally undergo DPCD^{9,32,34,35}. For example, mutation of the gene *mab-5*, a homeobox-containing transcription factor, whose family members play key roles in specifying the body plan and developmental cells' fates in all metazoans, results in loss of programmed cell death of two cells that normally die in

development. This effect is attributable to loss of the direct transcriptional activation of *egl-1* by binding of MAB-5 in complex with CEH-20 at the *egl-1* locus³⁵. Thus, the key regulators of *egl-1* expression in the remaining 123 cells are unknown and, to date, there have been no unbiased systematic genetic screens to identify genes that regulate induction of *egl-1*.

A major barrier to investigating the specification of DPCD is the difficulty of visualizing DPCD at the cellular level. If DPCD occurs normally, the dead cell is removed and cannot be studied. If DPCD is blocked, for example by partial or complete loss of function (lf) mutations in *egl-1* or *ced-3*, the cells normally undergoing DPCD survive as “undead” cells. However, these undead cells do not have a distinctive morphology and cannot be distinguished from normal cells. If we could reliably mark these cells, we would have a powerful tool that would enable us to do a wide variety of experiments.

For example, it is presently unknown whether *egl-1* is the initiating signal for all cells that undergo DPCD. Using a reporter that marks cells in which *egl-1* is expressed with GFP, we could image developing embryos and compare those cells marked by GFP to the cell lineages known to undergo DPCD, answering the question of whether *egl-1* is expressed in all cells undergoing DPCD, or whether some cells undergo DPCD independent of *egl-1* expression. Similarly, for the mutations that have been described to impair DPCD in a handful of cells, it is unknown whether these mutations might have broader effects in regulating DPCD. This assay would allow reproducible assessment of the spectrum of cells that are affected by each mutation.

Further, by marking and tracking undead cells, we can follow the fates of each individual cell to better understand the biology of why their survival has been selected against in worm development. By purifying these cells (for example, using fluorescence-activated cell sorting) we could do single-cell RNA sequencing to better understand the identity and function of the undead cells. *C. elegans* has an excellent map of the gene expression of every normal cell type³⁶. We could also investigate the fates of these undead cells, observing the type of cell they become, any subsequent divisions they may undergo, and whether these fates are variable or invariable among worms. While many undead cells appear to have neuronal cell features, such experiments would better define neuronal and non-neuronal fates adopted by undead cells^{3,34,37}.

Finally, we could do a forward mutagenesis screen for mutations that alter *egl-1* expression, as assessed by GFP signal. *egl-1* is normally expressed in the 131 undead cells. We hypothesize that this specific expression is the result of both activating and repressing transcriptional control. Thus, we would expect to recover mutants with altered patterns of GFP expression, both increased and decreased. These mutations would likely be due to loss of transcription factors that act at the *egl-1* locus. Relatively gross changes in GFP expression could be readily identified by manual examination of large cohorts of worms on plates; more subtle abnormalities might be best identified in an automated fashion by combining high-throughput, high-resolution imaging of worms coupled with automated worm sorting to pull out worms with altered patterns of immunofluorescence³⁸. Counter-screens would need to be done to exclude loss

of function mutations in *gfp* or *cre* (by sequencing these genes via targeted sequencing of PCR amplicons), which would also produce loss of GFP signal. These screens can identify dominant or neomorphic mutations as well as loss of function alleles. Mutagenesis could be performed with EMS, which produces a range of DNA alterations including substitutions and indels³⁹. Repeated rounds of outcrossing followed by selfing to reproduce the homozygous phenotype would eliminate most unlinked mutations, following which whole genome sequencing combined with other techniques could be used to identify the causal mutation in each mutant strain.

Design of a method to mark cells programmed to die.

We sought to design a method to produce a permanent mark on undead cells that are normally induced to die due to activation of transcription of *egl-1*. This assay needs to address several challenges. First, the assay needs to overcome the fact that expression of *egl-1* normally leads to cell death, which would leave behind no cells to inform what genes had been involved in the activation of *egl-1*. Second, *egl-1* may only be transiently expressed in cells during development, further complicating the experimental design—a direct reporter of *egl-1* expression may not capture the brief period of expression.

To address these issues, we sought to genetically prevent cell death by mutating *egl-1* or *ced-3*, two genes required for DPCD, thereby allowing survival of cells in which transcription of the *egl-1* locus had been induced. We further sought to permanently mark the cells in which transcription at the *egl-1* locus had

been activated. We presume this activation typically occurs by factors that directly or indirectly promote *egl-1* transcription by interaction with flanking regulatory sequences. Permanent marking of these undead cells could be achieved with a reporter gene that would be permanently expressed by even transient expression at the *egl-1* locus. This could be achieved with an indirect *egl-1* reporter, rather than the direct *egl-1* reporters used in previous studies^{32,35,40}. Our indirect *egl-1* reporter will require two components that make use of Cre-Lox recombination: the first is the *cre* coding region flanked by *egl-1* regulatory sequences, and the second is a ubiquitous promoter driving expression of a *gfp* gene that has been disrupted by LoxP sites. When the *egl-1* regulatory sequence drives even transient expression of Cre, these LoxP sites will permanently recombine such that expression of the *gfp* gene is constitutively driven by the ubiquitous promoter to produce a functional green fluorescent protein. Successfully engineering such a system would thus allow for a permanent visible marker of all cells in which *egl-1* is normally expressed.

Methods

Making a construct to replace the *egl-1* coding region with *cre* recombinase via CRISPR/Cas9

Segments extending from the transcription start site of *egl-1* to 60, 100, 300, or 1000 bases 5' to the start site were amplified from the genomic DNA flanking *egl-1* using specific PCR primers identified using *A plasmid Editor (ApE)* program. Segments of 60, 100, 300, or 1000 base pairs lying 3' to the end of the *egl-1*

coding region were similarly amplified and purified. These flanking sequences will provide sequences to direct homology-directed repair at the *egl-1* locus. A plasmid encoding *cre* recombinase (from Addgene) was used as a cloning vehicle. The plasmid was linearized at unique digestion sites either 5' or 3' to the coding sequence, and the amplified segments of *egl-1* regulatory regions were sequentially ligated onto the 5' end and 3' end of the *cre* coding sequence using DNA ligase, and the resulting clone bearing *cre* flanked by *egl-1* regulatory sequences was cloned in the same bacterial plasmid, purified, and the insert was liberated from the plasmid by restriction enzyme digestion and purified by agarose gel electrophoresis.

We used dominant markers for hygromycin resistance and the 'dumpy' phenotype (shorter, rounder worms) as co-injection markers. These were included in the injection mix and introduced as extrachromosomal arrays. This enabled visual identification of worms that had undergone germline transformation, which could then be further studied for successful CRISPR/Cas9 replacement at the *egl-1* locus.

Injection mix containing these constructs was injected into gonads of L4-stage worms, as described below.

Making a construct to replace the *egl-1* coding region with *Cre* recombinase via extrachromosomal array integration of a transgene.

For extrachromosomal linear array production, the same *Cre* construct was made, as described above, with the exception that the 5' flanking region

comprised 1 kb of DNA upstream of the *egl-1* transcription start site and the 3' flanking region comprised 5.8 kb of DNA 3' to the end of the *egl-1* transcription unit. These flanking regions have been shown to contain sequences critical for for proper regulation of the *egl-1* gene, although it is possible that additional regulatory sequences exist¹⁵. The resulting cloned construct was verified by the production of the predicted DNA fragments following digestion with restriction endonucleases, and the insert was excised from the plasmid and purified for injection by agarose gel electrophoresis.

We used the fluorescent protein mCherry under transcriptional control of the *myo-2* promoter, which is constitutively expressed in the pharyngeal muscle cells, as a co-injection marker. This was included in the injection mix and introduced as part of the extrachromosomal array that could subsequently be integrated. This enabled visual identification of worms that had undergone germline transformation, which could then be further studied for successful integration of the *egl-1/Cre* transgene.

Injection mix containing these constructs was injected into gonads of L4-stage worms, as described below.

Making a construct for CRE-dependent expression of GFP via extrachromosomal integration of a transgene.

A plasmid was obtained from Addgene containing the constitutive *his-71* promoter, followed by a rearranged *gfp* gene, in which exons 2 and 3 are inverted and flanked by LoxP sites that are in opposite orientation. As a result,

this construct will not make functional GFP. However, in the presence of Cre recombinase, homologous recombination between the two LoxP sites will produce the normal GFP open reading frame, resulting in production of functional GFP.

We used the fluorescent protein mCherry under transcriptional control of the *myo-2* promoter as a co-injection marker. This was included in the injection mix and introduced as part of the extrachromosomal array that could subsequently be integrated. This enabled visual identification of worms that had undergone germline transformation, which could then be further studied for successful integration of the *egl-1/Cre* transgene.

Injection mix containing these constructs was injected into gonads of L4-stage worms, as described below.

Worm injections

A PC-10 Puller from Narishige Group was used to generate needles from glass capillaries for microinjection of DNA into *C. elegans* gonads. L4-stage worms were mounted on injection pads and examined under 40x light microscopy to locate the gonad. The gonad was then positioned close to the tip of the needle at a perpendicular angle and the worm pushed into the needle until the needle tip entered the syncytium, penetrating through the cuticle and the layer of cells bordering the gonad. The injection mixture was then injected into the syncytium, creating a flow of liquid through the syncytium that can be observed to displace the nuclei. Using this technique, the anterior gonad, posterior gonad, or both can

be injected. We typically inject approximately 20 animals per session. After injections, animals were recovered in M9 and singled to a fresh NGM plate.

CRISPR/Cas9 editing

For CRISPR/Cas9 replacement of *egl-1* with *cre*, sgRNAs targeting the coding region of *egl-1* with an appropriate PAM site were identified and obtained from IDT. An injection mix of 50 ng/mL of pDD162 (*P_{eft-3}::Cas9*), 40 ng/mL of the *egl-1* sgRNA, 30 ng/mL per 50 nt dsDNA of repair template, 30 ng/mL of *dpy-10* sgRNA, and 26 ng/mL of *dpy-10* repair template, was used for injection into gonads of L4-stage worms.

F1 progenies of the injected parents were examined for *dpy-10* phenotype, and dumpy worms were subject to Sanger sequencing.

Integration of extrachromosomal arrays

As an alternative to precise genome editing, we also used the *egl-1/cre* construct and the Cre-dependent GFP construct to make extrachromosomal arrays in which the DNA constructs, without the sgRNAs, Cas9, or *tracr* RNA were injected as above.

Extrachromosomal DNAs can replicate and be maintained as stable arrays. However, they can also be integrated into the *C. elegans* genome by trimethylpsoralen (TMP) mutagenesis plus UV light, which induces double strand DNA breaks, with integration of constructs at breakage sites. For extrachromosomal array integration, transgenic animals were treated with TMP

solution and illuminated with 30mJ of 365nm UV light. To recover, concentrated OP50 was then added to the plates and the animals were stored in the dark for 2 hours or more.

Animals showing the pharyngeal mCherry phenotype were selected for evaluation of chromosomal integration of the constructs; expression of mCherry was taken as evidence of the presence of the transgene arrays.

Mapping integrants to specific chromosomes

Integration of the transgenes into chromosomes following TMP-UV treatment was tested by segregation analysis. Integration into a chromosome can be proved by mapping integrants to a specific chromosome via crossing transgene-bearing worms to mapping strains. In these experiments, mapping strains EG1000 and EG1020 were used, each of which bears three visible recessive phenotypes on different chromosomes; the two strains collectively mark all worm chromosomes, I – V and the X.

Worms presumptively homozygous for transgenic constructs were crossed with worms of the EG1000 and EG1020 strains that were homozygous for all three visible phenotypic markers. Resulting F1s were heterozygous at each of the visible marker loci and were confirmed to express mCherry by fluorescence microscopy. These worms were then selfed. In the resulting F2's, worms with each visible recessive phenotype were selected and immunofluorescence was performed to look for mCherry expression. In the absence of recombination, the presence of a visible recessive phenotype such as *dumpy* due to a mutation on

chromosome V should never be accompanied by mCherry fluorescence if *mCherry* is integrated to chromosome V, since both copies of chromosome V would have been inherited from the mapping strain and not from the strain bearing the *mCherry* gene. In contrast, if *mCherry* is integrated instead on a different chromosome (e.g., chromosome II), many worms with the *dumpy* phenotype will be positive for mCherry. Thus, anticorrelation of mCherry and a recessive phenotype known to lie on chromosome *n* provides clear evidence that mCherry lies on the homologous chromosome. This is further supported by finding that recessive phenotypes due to mutations on other chromosomes do not show such anticorrelation. Because recombination can occasionally occur in the interval between the site of mCherry integration and the location of the recessive mutation derived from the mapping strain, anticorrelation may not be perfect, but such apparent recombinants should be uncommon, given that none of the *C. elegans* chromosomes comprise more than about 50 centimorgans.

Animals

Wild-type inbred worms (N2), *ced-3* loss-of-function (MT1522) and mapping strains (EG1000 and EG1020) of *C. elegans* were used in this study.

Worm Maintenance

Worms were maintained on NGM plates seeded with OP50 bacteria. Active plates were maintained on the bench top, while master plates were stored in 15-

degree C and 20-degree C refrigerators. Transfer of worms to new plates was performed under a dissection microscope with platinum wire.

Induction of males

Spontaneous production of male progeny occurs at a low rate under normal conditions. When more male progeny were required, we transferred 5 L4 hermaphrodites of the desired line to new plates and heat shocked them at 34 degrees C for up to 4 hours. Highest yields of male progeny were produced from plates incubated at 34 degrees C for 135 minutes. These males can then be crossed with hermaphrodites of the desired strain to produce a stable population of males. Plating these worms at a higher ratio of males to hermaphrodites increases the likelihood of cross-fertilization over self-fertilization, and thus increases production of male progeny. A typical crossing plate might include 12 males and 4 hermaphrodites.

Freezing *C. elegans* using liquid freezing solution

Worms were frozen for indefinite storage in liquid nitrogen according to standard protocol⁴¹.

Visualization and imaging of worms for GFP fluorescence

Visualization and imaging of worms was done using fluorescence microscopy with the appropriate green and red filters for GFP and mCherry. Images were

captured using a spinning disk confocal microscope with worms mounted on 3% agarose pads and immobilized with 25mM Levamisole.

RESULTS

Project overview

Our goal was to introduce a permanent visible marker for DPCD. DPCD is normally initiated by expression of *egl-1*. Virtually all cells can be prevented from undergoing DPCD by making worms that are null for either *egl-1* or *ced-3*. Since all or nearly all cells that undergo DPCD uniquely express *egl-1*, we can use *egl-1* regulatory sequences to mark the resulting undead cells. A challenge in marking these cells is that, due to the transient expression of *egl-1*, a direct reporter of *egl-1* expression produces only a transient signal, limiting the scope of future experiments to which such a reporter could be employed. Previous attempts to build *egl-1* reporters result in marking of only a few of the 131 undead cells in *ced-3* mutants^{32,35,40}.

To solve this problem, we designed a two-component system in which the *egl-1* regulatory information drives expression of a gene whose expression in turn induces permanent expression of a reporter gene. A way of permanently turning on the expression of this reporter gene would be to induce a chromosomal rearrangement that creates an intact gene from one that was previously incapable of producing a normal protein product.

This can be accomplished by use of Cre-Lox recombination. The first component in our system will use *egl-1* cis-regulatory sequences to drive

expression of Cre recombinase, such that this enzyme will only be expressed in cells that normally express *egl-1*.

The second component comprises a constitutively active promoter ligated to the coding region of *gfp* in which several coding exons are in inverted orientation so that transcription cannot make the functional GFP protein. These inverted exons would be flanked by LoxP sites in opposite orientation to one another. In the absence of Cre, no functional GFP can be produced. However, if *cre* is expressed, it will induce homologous recombination between the LoxP sites, which will invert the orientation of the exons lying between the LoxP sites and restore an intact and functional GFP. This GFP would then be constitutively expressed, thereby providing a permanent mark of cells in which expression at the *egl-1* locus had been induced.

By combining these two components, even transient activation of the *egl-1* regulatory sequence in a cell will cause permanent expression of GFP, producing a visible marker of undead cells (Figure 2).

Design and construction of the *egl-1/cre* driver template for CRISPR

To build a Cre-Lox reporter strain for *egl-1*, we first sought to build the Cre driver component. This strain must be designed in such a way that expression of *cre* is driven by the regulatory sequence of *egl-1*. One approach to integration of this Cre driver component was to use CRISPR/Cas9 to precisely target a double-strand DNA break and homologous repair such that the coding region of *egl-1* was excised and replaced with the coding region of *cre*. This approach has the

advantage of simultaneously generating the loss of function mutation in *egl-1* that will abolish DPCD and of integrating the coding sequence of *cre* under transcriptional control of the endogenous *egl-1* regulatory sequence.

To this end, we made constructs in which homology arms—DNA identical to the genomic sequence immediately 5' and 3' of the *egl-1* transcription unit—of varying lengths (60bp, 100bp, 300bp and 1000bp) were ligated respectively to the 5' and 3' ends of the gene encoding Cre.

Attempted CRISPR engineering of the *egl-1* locus to express *cre*

We attempted to induce replacement of the *egl-1* coding sequence with the *cre* cassette by injecting wild-type (N2) *C. elegans* in the L4 developmental stage with a guide RNA targeting the coding sequence of *egl-1*, along with Cas9 protein and the linear fragment bearing the *cre* cassette flanked by 5' and 3' regulatory sequences from the *egl-1* locus, which would provide homology arms to enable homology-directed repair, as described in Methods (Figure 3). At the same time, co-injection markers for induction of hygromycin resistance and 'dumpy' phenotypes were injected as transgenes. In 14 rounds of injections, we injected a total of 296 worms, which we designated the P0 generation.

The F1 progeny were then scored for survival in the presence of hygromycin and for having the dumpy phenotype. These provided visible markers that germline transformation had occurred. We isolated 271 transgenic F1's originating from 64 P0s. Thus, germline transformation occurred in ~22% of

the injected P0s, and when transformation occurred, these P0s produced an average of ~4.23 transgenic F1 progenies each.

Transgenic F1s were then singled to fresh NGM plates and allowed to produce F2s. After producing F2s by hermaphrodite self-fertilization, the F1s were then individually lysed and their DNA amplified by PCR. To test replacement of *egl-1* with *cre*, a forward primer was located within the *cre* gene itself, while a reverse primer was located beyond the homology arm of the 3' end of the insertion construct, thus lying in the native *egl-1* locus. PCR amplification would then produce products of the proper size only if *cre* had replaced the *egl-1* gene at the native *egl-1* locus. The resulting PCR products were analyzed by gel electrophoresis for bands of appropriate length.

Altogether, we injected 296 worms, resulting in 64 germline transformations and leading to the production of 271 transgenic F1 progenies with the dumpy phenotype. We analyzed each of these F1s for *cre* integration and found no evidence for integration. In the course of these experiments, we tried modifying our protocol by varying the lengths of our homology arms, but we were never able to find evidence of *cre* integration. There are numerous possible explanations for the failure of this approach, which are elaborated in the Discussion.

Design and construction of the *egl-1/cre* driver gene for injection as a transgene

As an alternative approach, we sought to create transgenic worms by integration of extrachromosomal arrays rather than via CRISPR/Cas9. For CRISPR/Cas9 editing we only needed a construct with short homology arms flanking *egl-1* coding regions linked to *cre* in order to drive homology-directed repair to the endogenous *egl-1* locus, because once in place the *cre* sequence would be under transcriptional control of the endogenous *egl-1* locus. By contrast, for an extrachromosomal array, the construct needs to contain regulatory sequences flanking the *egl-1* locus in order to mimic endogenous *egl-1* expression. We therefore first identified the known cis-regulatory sequences for *egl-1*¹⁵. This comprised 1 kb of DNA 5' to the start of *egl-1* transcription and 5.8kb in the 3' UTR and beyond the end of the coding region. These sequences were produced by PCR and were then ligated respectively to the 5' and 3' ends of the *cre* coding sequence and purified from cloned constructs (Figure 4). *mCherry*, expressed from the *myo-2* promoter, was prepared for co-injection with this construct.

Generation of transgenic lines carrying the *egl-1/cre* construct as an extrachromosomal array

We injected the *egl-1/cre* construct, along with the dominant *mCherry* as a visible co-injection marker, into the gonads of 20 L4-stage *ced-3* loss-of-function mutant worms as described in Methods. After injections, we allowed these P0 worms to self-fertilize and produce progeny (F1s). We performed a visual screen for presence of the mCherry co-injection marker to identify worms bearing the extrachromosomal array in the F1 generation. We identified 65 transgenic F1s

originating from 9 P0s. We singled 15 transgenic F1s to fresh plates and scored their F2 progeny for percent expression of the mCherry marker. From these, we selected lines in which 30-70% of the worms carried the mCherry marker, presumably as an extrachromosomal array. Lines with this level of transgene maintenance were good candidates for attempts to integrate the arrays into chromosomes by induction of double strand breaks, as described in Methods.

Chromosomal integration of the extrachromosomal array *egl-1/Cre* construct

Following selection of these lines, 10 F2s from 3 lines were singled and expanded for mutagenesis of >100 worms in the F3 generation. Once these F3s reached the L4 developmental stage, they were mutagenized with trimethylpsoralen treatment and exposure to UV radiation, as described in Methods. This mutagenesis introduces random double-strand breaks to the DNA, providing a substrate for integration of the extrachromosomal array at these sites in the genomes of gametes by non-homologous end-joining. At the doses of mutagen used, it is expected that integration will not occur in most gametes, and that there will rarely be more than one integration event per genome. After recovering the mutagenized L4 worms, 10 of these L4s (now considered the P0 generation for the following experiments) were picked to each of 13 fresh master plates, where they produced progeny (F1s).

Plates were then stored in 20-degree C incubators and starved. When starved, *C. elegans* larvae arrest, either at the L1 stage—in which they remain

viable for a couple of weeks—or in an alternative ‘dauer’ stage—in which they remain viable for a couple of months. From each of these starved plates, a chunk approximately 25mm x 25mm of the NGM containing these larvae was then transferred to plates freshly seeded with OP50, and the worms allowed to reproduce. This process of starving, chunking, and reproducing was repeated once more. It is expected that among the resulting progeny will be marker-positive integrants heterozygous for the transgene, some marker-positive integrants homozygous for the transgene, and non-integrants that may yet exhibit marker positivity due to continued transmission of the extrachromosomal array.

From each of these plates, 20 marker-positive L4s were picked and singled, tracking from which master plate each worm derived. While it is possible to have more than one integration event among the 10 P0s originally picked to each master plate, because integration is a rare event, each population deriving from the 10 independent P0s picked to each of the 13 master plates likely contains no more than one integration event. We call the F1 animal that originally contained this integration the ‘founder’.

In addition to true integrants, some of the singled marker-positive L4s will merely contain the original extrachromosomal transgene. If that is the case, because the transgene is unstable, we expect that not all of their progeny will be transgenic. However, if chromosomal integration is present in the population, and if we pick an animal that is homozygous for the integrated transgene, 100% of the offspring of these worms will express the mCherry marker. We singled 260 worms deriving from 13 master plates. Screening of their offspring for those in

which 100% showed expression of mCherry demonstrated 17 putative integrants derived from 9 separate master plates. This provided evidence of multiple independent integrants for the *egl-1/cre* construct.

Generation of Cre-dependent GFP reporter strains

In parallel, we produced another construct in which the gene encoding GFP was ligated downstream of the ubiquitously active *his-71* promoter. As described in Methods, exons 2 and 3 of the gene were inverted and flanked by inverted LoxP sites. Thus, functional GFP cannot be produced from this construct, and will only be produced if Cre induces recombination between the two LoxP sites, flipping exons 2 and 3 into the proper orientation (Figures 5). As above, *mCherry* linked to the *myo-2* promoter was co-injected to provide a visible marker demonstrating germline transformation.

We injected this linear Cre-dependent GFP construct, along with the dominant *mCherry* as a visible co-injection marker, into the gonads of 20 L4-stage worms homozygous for the *ced-3* loss-of-function mutation, as described in Methods. After injections, we allowed these P0 worms to self-fertilize and produce progeny (F1s). Using the presence of the co-injection marker (mCherry) we performed a visual screen to determine successful introduction of our extrachromosomal array in the F1 generation, identifying 48 transgenic F1s originating from 7 P0s. 15 transgenic F1s were singled to fresh plates, and their F2 progeny were scored for percent expression of the mCherry marker. From these, we selected lines showing 30-70% stable transgenicity—ensuring enough

transgenic animals for subsequent integration by TMP mutagenesis, while still allowing for discrimination between possible integrants and extrachromosomal arrays.

Following selection of these lines, 10 F2s from 3 lines were singled and expanded for mutagenesis of >100 worms in the F3 generation. Once these F3s reached the L4 developmental stage, they were then mutagenized with TMP treatment and exposure to UV radiation as described in Methods. After recovering the mutagenized L4 worms (now considered the P0 generation in the following experiments), 10 of these L4 P0s were picked to each of 13 fresh master plates, where they were allowed to produce progeny.

Plates were then stored in 20-degree C incubators and starved. From these starved plates, a chunk of the NGM containing arrested larvae was then transferred to a set of freshly seeded plates, and the worms allowed to reproduce. This process of starving, chunking, and reproducing was repeated once more. From each of these plates, 20 L4s were singled, tracking from which master plate each worm derived.

We then examined the progeny of these singled animals, screening for plates in which 100% of progeny expressed the mCherry co-injection marker, consistent with the parent worm being homozygous for the transgene. Plates in which 100% of progeny were transgenic were considered putative homozygous integrants.

260 worms were singled from 13 master plates. Screening of the offspring of these 260 worms for 100% expression of mCherry demonstrated 19 putative

integrants derived from 6 separate master plates. This provided evidence of multiple independent integrants for our Cre-dependent GFP reporter.

Testing and mapping of integrants for *egl-1/cre*

Although 100% segregation of the transgene is strong evidence of chromosomal integration, it is possible that this is caused by extragenic stabilization of the array rather than integration. To confirm integration, we first assessed the behavior of each putative integrated transgene in an outcross. We expect that integrated transgenes will segregate in a Mendelian pattern, while extrachromosomal arrays will not. Putative homozygous integrants (P0s) identified above were crossed with wild-type N2 males. Transgenic male progeny of this cross (F1s) were then selected and crossed with wild-type N2 hermaphrodites. From the resulting F2s, there are three alternative outcomes. If the transgene is integrated on the X chromosome, we expect 100% of the mCherry positive progeny to be hermaphrodites, with zero males being mCherry positive. If the transgene is integrated onto an autosome, it will segregate independently of the X chromosome, so the proportion of mCherry positives that are males or hermaphrodites should not significantly deviate from 50% for each. In either case, the F2 hermaphrodites should be heterozygous and, when selfed, classic Mendelian proportions should be observed.

If the transgene array has not integrated, the results are more complex, because during meiosis in males (which have a single X and no Y), unintegrated transgenes often segregate away from the unpaired X, resulting in sperm that

either have an X or have the transgene, but not both. In this case, transgene positive offspring will be significantly more frequently male than hermaphrodite. Moreover, the finding that transgene positive worms are hermaphrodites less than 100% of the time excludes X linkage, while the finding that significantly fewer than 50% transgenic worms are hermaphrodites makes autosomal linkage unlikely, pointing to absence of integration of the transgene.

We performed this test by picking ~40 mCherry-positive progeny from nine F1 crosses and determined the number of males and hermaphrodites for each. The results of these studies identified 7 strains very likely to have integration of the *egl-1/cre* construct (Table 1). Five of these showed no significant departure from a 50-50 sex ratio among mCherry positive offspring by chi-square analysis, with no strong bias toward males, consistent with autosomal integration. Two showed 100% hermaphrodites among mCherry positives, consistent with X chromosome integration. The other two showed significantly more mCherry-positive males than hermaphrodites ($p = 0.0008$ and $p = 0.006$ by chi-square analysis), providing evidence of non-integration of the transgene array. These latter two lines were excluded from further analysis.

To confirm and extend these results, we performed genetic mapping of each integrant, with the goal of mapping it to a specific chromosome. This is important not just for establishing integration, but is critical for subsequent strain construction in which we seek to make triply homozygous worms for *ced-3* loss of function (*ced-3* is located near the end of chromosome IV, allowing for recombinant events with transgenes on chromosome IV), the *egl-1-cre* transgene,

and the Cre-dependent GFP transgene. Having our transgenes on separate chromosomes is essential to making the triply homozygous strains by simple crosses.

We performed a mapping experiment using the mapping strains EG1000 and EG1020, as described in Methods. Each mapping strain contains three recessive mutations resulting in three visible phenotypes. Each mutation is on a different chromosome, and thus the two strains collectively the six *C. elegans* chromosomes, autosomes I - V and the X chromosome. The first step of mapping is to cross the mapping strain with the integration to be mapped. The resulting F1 animals will be compound heterozygotes. For the chromosome that the integration is on, one homolog will have a mapping mutation and the other will have the integration. When these F1s are selfed, the recessive phenotype corresponding to that mapping mutation should be significantly anticorrelated with the presence of the integrated mCherry transgene. If integration has occurred on, for example, chromosome V, nearly all worms with a recessive visible phenotype due to mutation of a gene on chromosome V should almost always be mCherry negative, with the only exceptions being meiotic recombinants. In contrast, if the integrant is not on chromosome V, worms with a recessive visible phenotype due to mutation of a gene on chromosome V should, on average, be mCherry positive 75% of the time (since *mCherry* is heterozygous in the self-fertilizing parent).

The seven putative homozygous integrant strains were crossed with each of the two mapping strains to produce F1 offspring heterozygous at each test

locus. F1s were then selfed to produce F2s. Worms with visible recessive phenotypes from each selfing were selected, and expression of *mCherry* was evaluated by fluorescence microscopy. To have sufficient power to map putative integrants, for each cross we sought to produce an average of 30 worms with clear evidence of each visible recessive marker, and then scored the presence or absence of the mCherry marker in each. This typically entailed the screening of several hundred offspring of each cross to identify the desired number of worms with each visible recessive phenotype, with a cross to each of the two mapping strains for each putative autosome integrant, and a cross to the EG1020 strain for each putative sex chromosome integrant.

The presence or absence of mCherry was determined in worms with each of the recessive visible markers for all seven strains tested, and the results are shown in Table 2. The results demonstrate clear evidence of independent integrants, with autosomal integrants showing far less than the 75% mCherry positivity expected by chance. The results showed one integrant on chromosome II, two on chromosome V, and one on the X chromosome. The remaining two strains showed no significant evidence of integration on any chromosome.

An illustrative example is the strain from master plate 4.16. In this cross (Table 2), 30 worms were scored that had the visible recessive dumpy phenotype due to mutation on chromosome V. 29 of these did not have the mCherry phenotype, whereas only one did (3% mCherry positive). This is a highly significant departure from the 75% mCherry positivity expected if mCherry were on a different chromosome (chi square, 1df = 82.1, $p < 0.00001$). In contrast,

none of the other chromosomes showed a significant departure from the expected occurrence of mCherry in conjunction with a recessive visible phenotype. Moreover, in this same line (4.16) among all chromosomes other than chromosome V, mCherry was collectively found in 114 of 148 worms with recessive visible phenotypes (77%), very close to the expected value of 111 (75%). These results collectively provide extremely strong evidence of integration of the transgenic array to a single chromosome, chromosome V. Similar results were found for the three other mapped integrants on chromosomes II, V and X, while there was no strong evidence of integration for the three other tested lines.

Testing and mapping of putative integrants for Cre-dependent GFP constructs.

Analogous analysis testing for integration and mapping of integrants for the Cre-dependent GFP construct was performed as was done for the *egl-1/cre* construct. Six strains putatively homozygous for this transgene, as identified above, were crossed with wild-type N2 males. Male progeny of this cross (F1s) were then selected and crossed with wild-type N2 hermaphrodites. ~40 mCherry-positive progenies were scored for their sex. The results are shown in Table 3. In one line, 100% of mCherry-positive worms were hermaphrodites, providing evidence of integration on the X chromosome. Three lines showed no significant departure from an equal sex ratio among mCherry-positive progeny, suggestive of autosomal linkage. The other two lines showed a strong but incomplete bias toward male gender among mCherry-positive progeny (89% and

77%), effectively excluding linkage to either the X chromosome or autosomes. These latter two strains were excluded from further analysis as being likely non-integrants.

The four remaining promising lines were crossed to the mapping strains and analyzed as described above. The results are shown in Table 4. We identified three independent integrants, one each on chromosomes II, IV and X, with one line not providing significant evidence of integration.

The results of these experiments identified independent integrants of both transgenes, with integration occurring on sufficiently diverse chromosomes that worms simultaneously homozygous for *ced-3* loss of function, the *egl-1/cre* construct, and the Cre-dependent GFP construct can be made by simple crosses.

Recovery of worms triply homozygous for transgenic *egl-1/cre*, transgenic Cre-dependent GFP and *ced-3* loss of function.

Outcrossing while selecting for our desired transgenes has the benefit of decreasing the frequency of deleterious mutations that might have occurred as a consequence of TMP mutagenesis, and which may decrease the viability of the animals. Each of our putative integrants was outcrossed twice with the wild-type N2 strain, and each strain that demonstrated integration by mapping was outcrossed twice more with a *ced-3* knockout strain.

A consequence of outcrossing was loss of homozygosity of our integrated transgenes and of the *ced-3* mutation. Therefore, after successful outcrossing,

we performed crosses to produce worms that were triple homozygotes for *egl-1/cre*, Cre-dependent GFP, and the *ced-3* mutation. We started by selfing worms that were doubly heterozygous for *egl-1/cre* and *ced-3* on different chromosomes. It was expected that 1/16 (~6%) of the F1 offspring would be homozygous at both loci. To identify these, individual F1 worms were selfed and their progeny were first screened for broods in which 100% expressed the visible marker mCherry linked to the *egl-1/cre* locus, which will only occur if the F1 parent was homozygous at the *egl-1/cre* locus. This result was found in about 25% of the progeny of selfed F1's, consistent with expectation.

These *egl-1/cre* worms were selected and selfed again and screened by PCR for worms whose offspring were all homozygous for the *ced-3* mutation. Genotypes at *ced-3* were determined by amplification of the segment of *ced-3* that contains the null mutation, which destroys an ApE-KI restriction endonuclease cleavage site. Thus, digestion of the segment following PCR will produce a wild-type product that is cut into two fragments by ApE-KI, but a mutant product that will not be cut. This allows ready discrimination of homozygous wild-type, homozygous mutant, and heterozygous worms. Offspring of worms that are either homozygous mutant or heterozygous will produce either 100% homozygous mutant offspring or offspring that are 75% non-homozygous mutant. Thus, by genotyping four offspring of each selfing worm, finding that all are homozygous mutant for *ced-3* provided strong evidence that the parent was homozygous mutant, since this result is 256-fold more likely to have resulted from a homozygous mutant parent than a heterozygous parent (odds ratio

1/(1/4)⁴). This effort identified many clones that were doubly homozygous for the *egl-1/cre* transgene and *ced-3* mutation (Figure 6).

To produce worms that were also homozygous at the Cre-dependent GFP locus, worms that were homozygous at this locus were produced in parallel by the analogous approach above, using the linked *mCherry* as a visible marker. This identified F2 offspring that, when selfed, produced 100% *mCherry* positive worms. These two homozygous lines were then crossed with one another, selfed, and their progeny screened for lines that only produced worms homozygous at all three loci. We ultimately made triply homozygous lines with all possible pairs of sites of integration of each of the two transgenic insertions, resulting in 10 genetically distinct permutations.

Expression of GFP

The test for the efficacy of our genetic engineering of these lines was to look for GFP expression in triply homozygous worms. GFP should only be expressed if *ced-3* is homozygous mutant, thereby producing undead cells, AND Cre is expressed under *egl-1* regulatory control, AND Cre expression produces rearrangement at the Cre-dependent GFP locus. Importantly, if worms are homozygous at all three loci, 100% of the progeny of selfing should express GFP.

Figures 7 and 8 show the results. In the absence of these constructs, worms show no significant green fluorescence signal other than in gut granules. In preliminary examination of two independent triply homozygous lines, all worms

showed many cells expressing GFP in the head. These are concentrated in green fluorescence-tagged cells in the posterior bulb, which includes the densely innervated head ganglion, as well as more rostral cells in the isthmus and corpus. These preliminary results provide evidence that the desired strains have been made, and that both transgene constructs function as expected.

Induction of males and freezing of final strains

From strains triply homozygous for *egl-1/cre*, Cre-dependent GFP, and *ced-3* mutation, stage L4 worms were picked and heat shocked to generate males that could be used for crosses in future experiments. These strains were then either plated for immediate use or short-term storage in a 15-degree C incubator, or frozen to be stored indefinitely in a -80-degree C freezer and in liquid nitrogen for future experiments.

Discussion

The biochemical pathway that produces programmed cell death in the development of *C. elegans* is well-defined; however, the upstream regulators of *egl-1*—the gene that initiates the process—are largely unknown. We have engineered the genome of the worm *C. elegans* to devise a method that can be used to visualize undead cells. This system could provide the foundation for studies of undead cell lineage and function, as well as genetic screens to identify genes responsible for the induction of *egl-1*, which would be an important step toward a complete understanding of how cells are specified for programmed cell

death. Because the programmed cell death pathway is highly conserved among all animals, including humans, understanding the regulators of this process in *C. elegans* can provide important insights into the fundamental biology regulating this process.

In our experiments, we introduced two transgene cassettes by germline injection into a strain of *C. elegans* homozygous for a *ced-3* loss-of-function mutation, such that cells do not undergo programmed cell death in development. One cassette links the 5' and 3' regulatory elements that flank the normal *egl-1* gene to *cre* recombinase, while the other has a green fluorescent protein (GFP) reporter that is permanently expressed by genomic rearrangement if Cre is even transiently expressed. These cassettes were transmitted to progeny as stable extrachromosomal arrays, then randomly integrated to chromosomes by TMP/UV mutagenesis, as confirmed by segregation/co-segregation data in our mapping experiments.

We succeeded in producing four independent genomic insertions of the *egl-1/cre* cassette and three with the Cre-dependent GFP cassette. We made 10 strains that had different combinations of the *egl-1/cre* and Cre-dependent GFP cassettes and made each triply homozygous for these plus the *ced-3* loss-of-function mutation. Preliminary work provided evidence of Cre-dependent expression of GFP in two of these lines. These preliminary results suggest that GFP expression reproducibly labels many cells in the worm's head, specifically in the posterior bulb, the isthmus, and the corpus, with no reproducible signal identified in posterior structures.

Challenges

The mapping strategy used to demonstrate independent chromosomal integrants was very successful. Nonetheless, a number of crosses and production of many progeny was required to map each locus. In the time since this work was performed, longer-read genomic DNA sequencing has become more available and less expensive, suggesting use of brute-force genomic sequencing to identify chromosomal integrants may be preferable. Long reads can be done by, for example, PacBio sequencing, employing highly processive polymerases that can read the same sequence repeatedly to routinely achieve ensemble consensus reads that are highly accurate, with read lengths of 10s of thousands of base pairs⁴². These long reads are sufficient to unequivocally identify the sequence joining integrants to chromosomal DNA, enabling rapid assessment of integration sites at base-pair resolution. An additional benefit is the ability to determine whether there are companion mutations that might be deleterious. Because TMP/UV mutagenesis creates insertion-deletion mutations, they can be readily identified with high-quality sequence, and the inference as to whether mutations in coding regions are functionally significant is considerably clearer for insertion/deletion mutations than for induced point mutations. The small size of the *C. elegans* genome gives this or analogous approaches (e.g., “10x fragmentation” sequencing⁴³ or nanopore sequencing—in which single bases are read as they are drawn through a pore, such as occurs when DNA is packaged into a viral capsid)⁴⁴ the potential to permit direct identification of integrants

without the time required for performance of the crosses needed for analysis of co-segregation.

While our efforts at genetic engineering ultimately proved successful using extrachromosomal array integration, we initially attempted to use the CRISPR/Cas9 system for this purpose. The reason our CRISPR/Cas9 editing was unsuccessful is not entirely clear. In these experiments, because not all injections will produce germline transformation, it is highly useful to have a concurrent positive control for germline transformation—if this DNA has entered the germline and been transmitted to an offspring, other co-injected DNAs are empirically highly likely to have accessed the same germline nuclei. If this positive control can be scored by visible inspection of the worm, one can readily focus on these worms to assess whether the desired correction introducing *cre* into the germline has occurred. In our CRISPR experiments, the dominant marker *dpy-10* proved to be very useful as an independent marker of transformation, indicating that injected DNA was reaching the nucleus of germline cells. Because we produced many progenies exhibiting the ‘dumpy’ phenotype, we can be confident that our CRISPR cassette was reaching the germline, and that failure to do so was not the cause of our apparent failure to achieve successful repair with our *cre* template.

Ultimately, the cause of this failure eludes us. While the length of the non-homologous sequence being inserted was longer than, for example, a very short ‘patch’ carrying a desired homologous insertion, insertions as long as the one we sought to make have been successfully inserted into the worm genome, though

with low efficiency. Nonetheless, achieving the needed molar concentration of a construct several kilobases in length versus one only 30 base pairs in length could make success harder to achieve, particularly with a long segment of non-homology. Another potential explanation for this failure could be biological. It is possible that complete loss of function for *egl-1* might be lethal or severely impair reproductive fitness. To this point, Horvitz and colleagues noted in their 1998 paper describing the cloning of *egl-1* that complete nulls for this gene had never been discovered and loss of function mutations identified in genetic screens had never been clear nulls, i.e., deletions, frameshifts or premature termination mutations, suggesting these could, in fact, be lethal¹⁵.

Future experiments

Chromosome engineering in *C. elegans* is clearly extremely powerful, permitting complex manipulation of genes and regulatory elements to allow increasingly incisive questions to be asked about the regulation of fundamental biological processes such as developmental programmed cell death.

In our experiments, we sought to create a system that would permit large-scale, unbiased screening for mutations that fail to normally induce expression of *egl-1*, a gene whose expression normally initiates a cascade of events that result in programmed cell death of particular cells in development. The signals that induce *egl-1* expression are largely unknown, leaving open the question of how the system is programmed and controlled. This is an important question both because of the role of DPCD in vertebrate development—for example in

modeling distinct digits from an otherwise webbed hand or foot⁴⁵—and because of the role disruptions to the cell death pathway play in human pathology—for example, understanding how to induce apoptosis in cancer cells that often are protected from apoptosis via overexpression of Bcl-2⁴⁶ (a *ced-9* homolog) could be of clinical use. Genetic manipulation of *C. elegans* is extremely well-suited for dissecting the regulation of programmed cell death owing to the ease of genetic manipulation, small genome size with few paralogs of most genes, and short generation time with ability to produce and score phenotypes in hundreds to thousands of worms.

The next steps envisioned would be to characterize the cells that are reproducibly labeled by GFP in independent strains. Our preliminary work identified many cells in the head; autofluorescence in gut granules made an assessment of posterior structures more challenging. The lineage of each of the undead cells identified should be traced, permitting determination of whether all the marked cells are cells that normally die in development. Imaging of developing embryos using a dual-view inverted selective plane illumination microscope (diSPIM) that allows for volumetric time-lapse imaging can be performed, employing annotation software to map the lineage of the cells throughout embryonic development. This data can be used to determine where in the cell lineage GFP expression is activated, and whether it is present in all cells known to undergo programmed cell death.

Finding that marked cells comprise all 131 cells that normally undergo DPCD and no others would clearly implicate *egl-1* expression in all DPCD, while

labeling of a subset of these cells would indicate that there are likely be other pathways for activation of DPCD. Expression of GFP outside the 131 ‘developmental undead cells’ could occur for several reasons. First, Cre expression could be ‘leaky’ – expressed for reasons other than induction by *egl-1* regulatory sequences. This could occur as a consequence of the location of insertion into the genome; for example, *Cre* could be expressed under the influence of other nearby regulatory sequences. In this case, we would expect the result to vary in strains with independent insertions of the *egl-1/cre* cassette in different chromosomal locations. Second, studying post-embryonic or adult worms could increase the number of ‘undead’ cells beyond the 131 developmentally targeted cells, as could occur via induction of apoptosis due to stochastic damage. This is a consequence of the *ced-3* mutation, which would result in all cells induced to undergo apoptosis to become ‘undead’; expression of *egl-1* in any of these would cause them to be labeled with GFP. These additional apoptotic events could accumulate over the life of the worm. Consequently, studying worms at earlier stages would likely better restrict the signal to developmentally undead cells. This would be feasible, since 118 of the cells that are programmed to die in development do so during embryogenesis, while 13 die in post-embryonic development⁴⁷.

For the most promising strains, the final constructs could be readily verified by whole genome sequencing using long-read technology, as with PacBio sequencing; this would enable capture of the boundaries between insertions and flanking genomic DNA and identify any peculiarities to the

insertion events (e.g., other local genomic alterations). Determining the number of developmentally undead cells that are reproducibly labeled would be important to understand in considering going forward with a mutagenic screen to identify mutations that alter the pattern.

Projects that could be immediately pursued from having a large set of undead cells marked with GFP would include characterization of the cell types of each of the undead cells. Many, but not all of these are believed to be neurons. Now that there is comprehensive single-cell transcriptome data on *C. elegans* cells, and combinatorial indexing has made production of large single-cell transcriptome data sets inexpensive, isolating GFP-labeled cells by fluorescence-activated cell sorting followed by single-cell sequencing would rapidly allow characterization of the cell type of each undead cell³⁶. This could provide insight into their normal function and why they are always specified to die (i.e., what function do they provide that is eliminated by their death). Insight into this functional question can also be pursued by simply following the fate of these undead cells that have lineage tracing.

Similarly, because of the challenge in past efforts to identify and follow all cells that normally undergo DPCD, mutations that have been shown to impair DPCD of a small number of cells could be involved in DPCD of other cells that were simply missed in prior analyses. Having a visible marker for all undead cells would greatly simplify the study of the production of specific undead cells when, for example, a transcription factor used in some cells to activate *egl-1* is mutated.

Returning to a long-term goal of the project—to proceed to systematic TMP-UV mutagenesis to identify novel genes whose mutation would eliminate the signal from undead cells or reproducibly cause aberrant signal in cells that do not typically undergo programmed cell death. This is a challenging project, as it would require being able to score individual undead cells as being positive or negative for expression of GFP. If this was feasible, mutagenesis with TMP-UV in a highly inbred genetic background would be ideal for making and identifying mutations. Because the TMP mutagen makes small to medium-sized deletions, once phenotypic mutants have been identified that reproducibly knock out expression of reporter GFP in one or more undead cell types, the mutated gene could be quickly identified by brute-force whole-genome sequencing of worms with the mutant phenotype. Mutations that substantially and reproducibly reduce the number of undead cells produced in an embryo would likely be easiest to recognize; the robustness and consistency of labeling of undead cells in development would determine the level of resolution the mutagenesis approach could have. Because experiments are done in an inbred background, the sequencing of the starting strain should ostensibly be invariant, and, by sequencing a small number of segregants, the finding of the same mutation in worms that share the same mutant phenotype would provide strong evidence linking mutant genotype to mutant phenotype. From this starting point, this mutation could be studied in the wild-type background to demonstrate unequivocally which specific cells that normally undergo programmed cell death in development fail to undergo apoptosis, proving the relevance of the mutation.

Important to this effort would be optimizing the dosage of mutagen so that sufficient numbers of interesting mutations are produced, but not so large that mutagenized worms frequently have impaired reproductive fitness, and also a small enough number that outcrossing the mutants can eliminate a sufficiently large number of background mutants that sequencing of even a few related progenies that share the mutant phenotype will share only one or a small number of candidate mutations. These could readily be confirmed as causally related to the observed phenotype by making independent CRISPR/Cas9 knockouts of the mutated gene and assaying the effect on GFP expression in undead cells.

If the mutated genes identified proved to be transcription factors, then their mechanism of *egl-1* regulation could be further elucidated by identifying their DNA binding sites, either by searching for the presence of cognate binding motifs at the *egl-1* locus for that transcription factor, if they are known, or by performing ChIP-Seq on developing embryos to identify DNA sequences bound by the transcription factor. Binding sites will then be confirmed as *egl-1* cis-acting regulatory elements by editing their sequence using CRISPR and measuring its effect on *egl-1* expression using the *egl-1* reporter system. Other types of regulatory factors (e.g., histone modifying enzymes, microRNAs) would require analysis tailored to the specific gene products at each mutated locus. From these starting points, determination of the mechanism that produces expression of the identified gene in cells programmed to die would be of interest. Given that many of these are neurons, it would be of interest to study whether neuronal

firing or other distinctive aspects of neuronal function are drivers of activation of programmed cell death.

Figure 1

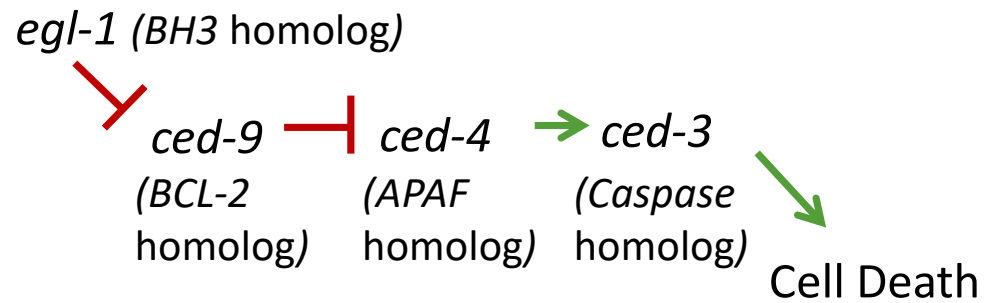


Figure 1. The *C. elegans* apoptosis pathway. The *C. elegans* genes in the canonical programmed cell death pathway are indicated, and the paralogous gene families that carry out the same functions that are found in humans and other metazoans are indicated in parentheses. Expression of *egl-1* is rate-limiting for activation of apoptosis. Its expression inhibits activity of *ced-9*, which normally prevents *ced-4* from activating the caspase protease *ced-3*, which in turn activates proteases and nucleases that produce cell death.

Figure 2

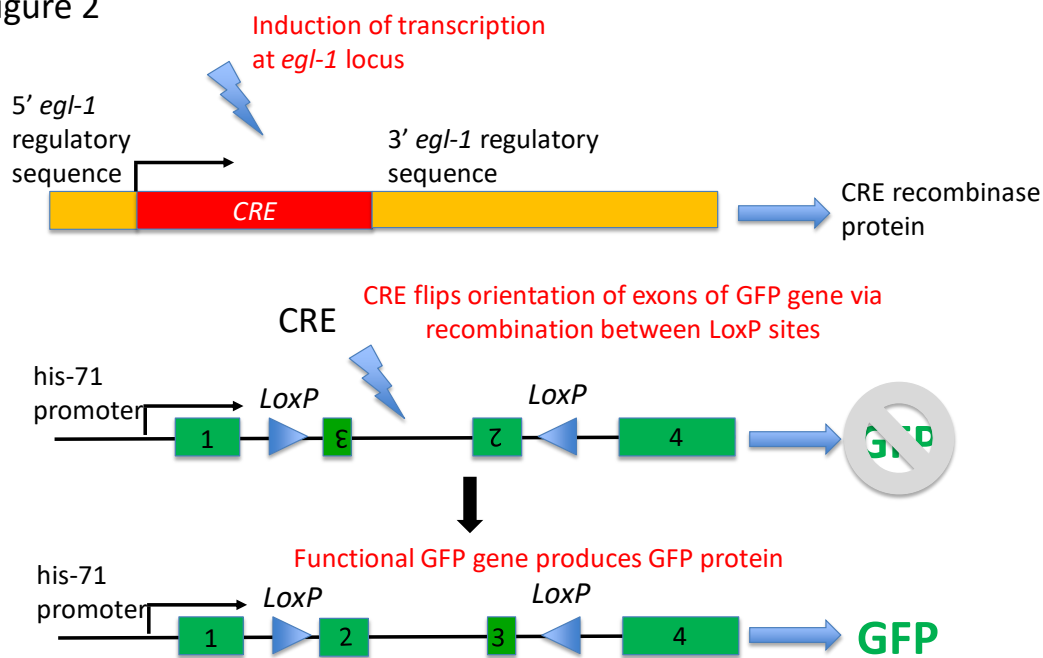


Figure 2. Marking undead cells with GFP. A schematic of the assay engineered to permanently mark 'undead' cells is shown. Induction of transcription via normal regulators of expression at the *egl-1* locus leads to production of mRNA encoding the CRE recombinase protein. CRE recombinase then induces recombination between inverted *LoxP* sites, flipping the orientation of exons 2 and 3 of the GFP gene to their correct, in-frame orientation. This gene is constitutively expressed under control of the *his-71* promoter, thereby continuously producing GFP. Cells expressing GFP are readily identified by their bright green immunofluorescence. This assay thus provides a permanent GFP mark in cells in which the normal transcriptional program for induction of *egl-1* was activated. Because the pathway for EGL-1-induced cell death is blocked by mutation of *ced3*, cells that normally die by DPCD survive as 'undead' cells and are selectively and permanently marked by GFP.

Figure 3

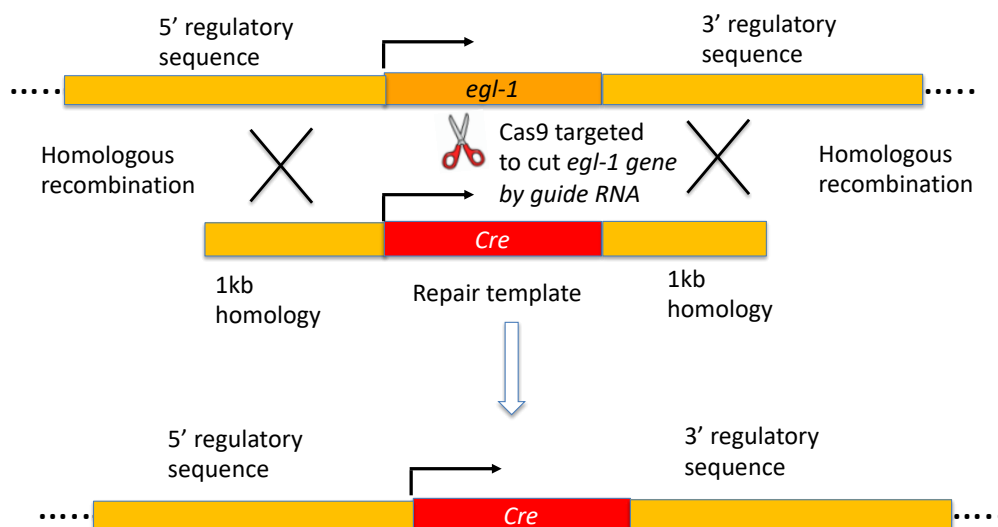


Figure 3. Design of CRISPR/Cas9 approach to putting *Cre recombinase* under control of *egl-1* regulatory elements. At the top of the figure, the general structure of the genomic *egl-1* locus is depicted, with the coding region flanked by 5' and 3' regulatory elements. Below, a replacement cassette in which the coding sequence of *Cre recombinase* has been ligated to the 1kb of sequence that lies immediately upstream and downstream of the *egl-1* locus is shown. This cassette, along with a 20 base guide RNA homologous to *egl-1* coding region that directs the Cas9 endonuclease (along with Tracr RNA) to make a double stranded cut in *egl-1* coding region, is injected into the gonad of L4-stage worms. Recombination between the homologous sequences 5' and 3' of the genomic *egl-1* locus and those of the repair template encoding CRE replace the *egl-1* coding sequence with *cre*.

Figure 4

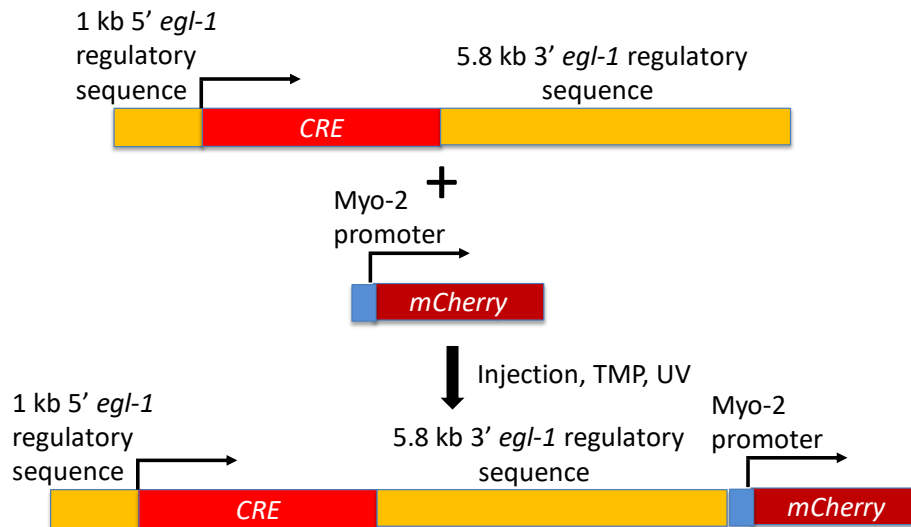


Figure 4. Design of extrachromosomal array putting Cre under control of *egl-1* regulatory sequences with mCherry. The coding region of the Cre gene has been ligated to 1 kb of 5' flanking sequence upstream of the *egl-1* coding region, and 5.8 kb of 3' flanking sequence distal to the *egl-1* coding region. The resulting fragment was cloned into bacterial plasmids, grown and the construct liberated by restriction endonuclease digestion and purified by gel electrophoresis. The mCherry gene linked to the myo-2 promoter was similarly purified. These were injected together into the gonads of L4-stage worms. Putative transformants were identified by mCherry fluorescence; these worms were treated with trimethylpsoralen plus UV light to induce chromosomal integration.

Figure 5

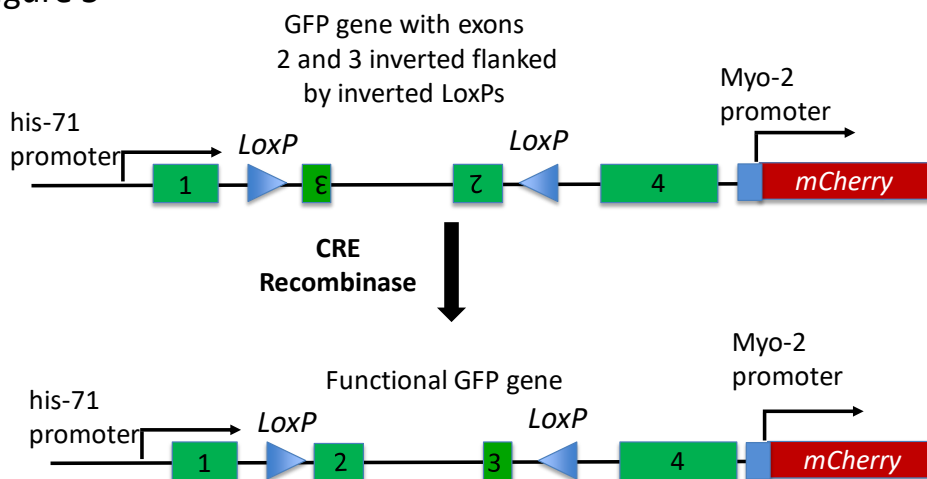


Figure 5. Design of extrachromosomal array with Cre-dependent GFP and mCherry. A plasmid insert containing the GFP gene with exons 2 and 3 in inverted orientation flanked by LoxP sites in inverted orientation was purified and injected into gonads of L4 stage worms along with the mCherry gene expressed under control of the myo-2 promoter. Putative transformants were identified by mCherry fluorescence and treated with trimethylpsoralen plus UV light to induce chromosomal integration of the array. In worms bearing this array, cells that express Cre recombinase will produce recombination between LoxP sites, flipping exons 2 and 3 to produce a functional GFP gene that will be constitutively expressed from the linked his-71 promoter.

Figure 6

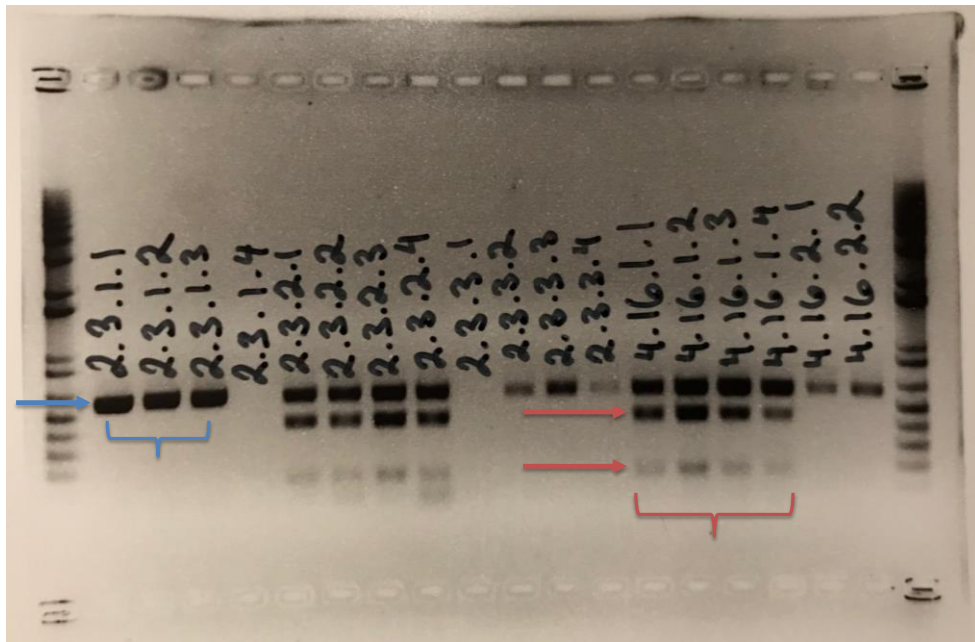


Figure 6. Determination of wild-type and loss of function alleles of *ced-3*. Wild-type and loss of function alleles of *ced-3* can be distinguished by the respective presence or absence of a cleavage site for the restriction enzyme ApE-KI that is abolished by the *ced-3* loss of function mutation. PCR amplification of a segment of the coding region that includes the segment bearing the ApE-KI site, followed by treatment with the ApE-KI enzyme, produces two fragments from wild-type alleles (red arrows) and the uncut product from the mutant *ced-3* (blue arrows). The genotype of a worm can be determined by analysis of agarose gel electrophoresis of the products of digestion of these PCR amplicons. The figure shows a gel of such products from 18 worms. The presence of a single large band in a column signifies a worm homozygous for the mutant *ced-3* (blue bracket), while the presence of all three bands in a column signifies a worm heterozygous for mutant and wild-type *ced-3*. (red bracket)

Figure 7

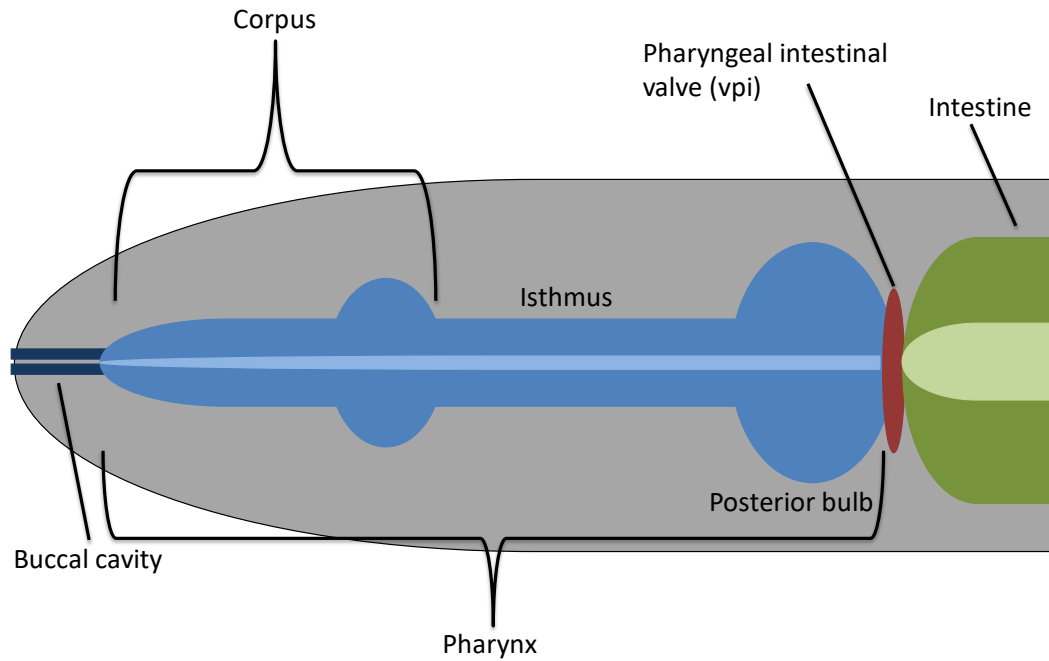


Figure 7. Anatomy and Nervous System of *C. elegans*.

A. Graphic representation of the anatomy of the *C. elegans* head. At the anterior end, the pharynx is connected to the buccal cavity. At the posterior end, it is connected to the intestine through the pharyngeal-intestinal valve (vpi). The posterior bulb contains dorsal, ventral, and lateral ganglia. Image adapted from Worm Atlas (www.wormatlas.org).

Figure 8

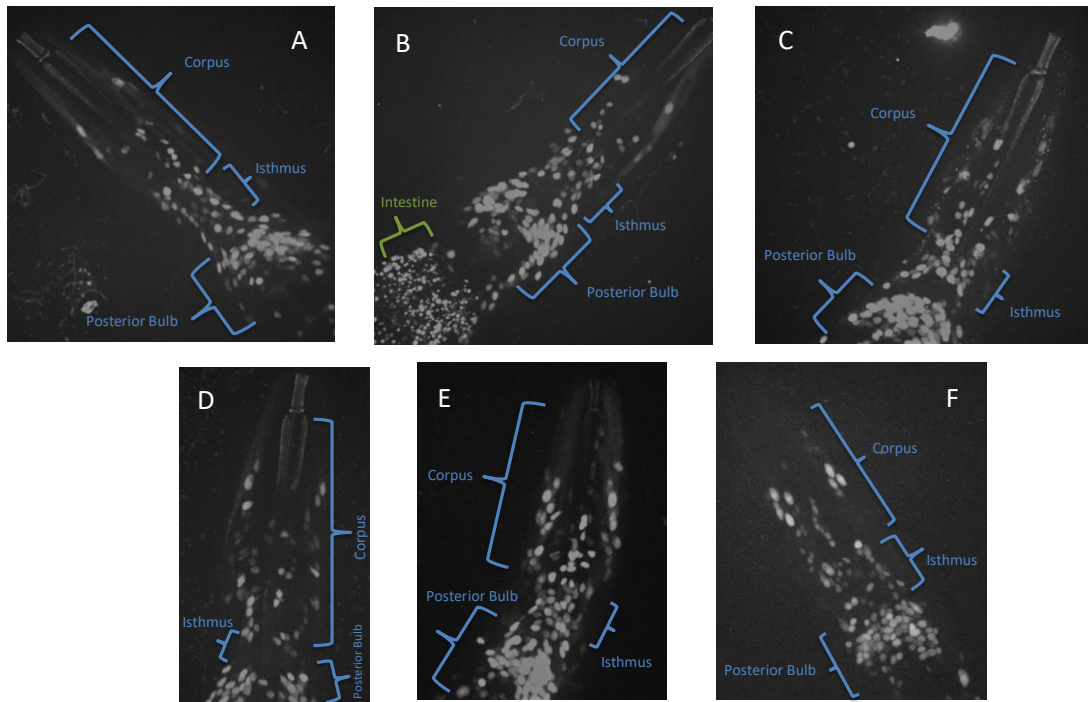


Figure 8. GFP expression in L4-stage *C. elegans* homozygous for *egl-1/Cre*; *Cre*-dependent GFP; *ced-3* lf mutant. Pictured are *C. elegans* homozygotes for *egl-1/Cre*; *Cre*-dependent GFP; *ced-3* lf mutant in the L4 developmental stage imaged under a green fluorescent filter. Images capture the anatomic regions from the buccal cavity to the pharyngeal-intestinal valve (vpi). Each image is a merged Z-stack of a unique animal. Images A through D originate from Line 1 (*egl-1/Cre* 4.16 x *Cre*-dependent GFP 5.14), and images E and F originate from the genetically independent Line 2 (*egl-1/Cre* 11.6 x *Cre*-dependent GFP 8.2). We observe a reproducible pattern of GFP signal in cells of the posterior bulb and corpus, with particularly high signal in the posterior bulb, where the dorsal, ventral, and lateral ganglia are located. The presence of auto-fluorescent “gut granules” are abundant in the intestine, seen in image B. There were no obvious cells distal to the pharyngeal-intestinal valve that were reproducibly labeled.

Table 1. Characterization of putative *egl-1/cre* integrants crossed with N2 wts

<i>egl-1/Cre</i> Plate #	Total # Transgenic	# Transgenic Males (% of Total)	# Transgenic Hermaphrodites (% of Total)	Interpretation
*2.3	40	23 (57.5%)	17 (42.5%)	Putative Autosome Integrant
*3.8	38	20 (52.6%)	18 (47.4%)	Putative Autosome Integrant
*4.16	38	14 (36.8%)	24 (63.2%)	Putative Autosome Integrant
*9.7	33	12 (38.7%)	21 (63.3%)	Putative Autosome Integrant
9.10	36.00	28 (77.8%)	8 (22.2%)	Putative Stable Array
9.16	34	25 (73.5%)	9 (26.5%)	Putative Stable Array
*10.12	30	0 (0%)	30 (100%)	Putative Sex Chromosome Integrant
*11.6	19	10 (52.6%)	9 (47.4%)	Putative Autosome Integrant
*11.16	30	0 (0%)	30 (100%)	Putative Sex Chromosome Integrant

Putative homozygous integrants (P0s) were crossed with wild-type N2 males. Transgenic male progeny of this cross (F1s) were then selected and crossed with wild-type N2 hermaphrodites. mCherry-positive progenies from each of the nine F1 crosses were picked and scored for percent males and percent hermaphrodites. Results are shown in the above table. 100% of mCherry-positive progeny being hermaphrodites indicates a likely integration on the X chromosome. Approximately 50% transgenic progenies being male and 50% hermaphrodites indicates a likely integration on an autosome. Transgenic progeny that are significantly more male than hermaphrodites likely indicates a stable array that has not integrated on a chromosome. * connotes putative integrants selected for confirmatory mapping by crossing with strains EG1000 and EG1020.

Table 2. Identification and mapping of *egl-1/cre* integrants

Master Plate #		Mapping Strain EG1000			Mapping Strain EG1020			Interpretation
		Dumpy (chr. I)	Roll (chr. II)	Long (chr. III)	Blister (chr. IV)	Dumpy (chr. V)	Long (chr. X)	
4.16	mCherry +	20	27	9	29	1	29	Integrated on Chr. V
	mCherry -	8	5	8	1	29	12	
2.3	mCherry +	17	9	12	13	16	8	Not integrated
	mCherry -	17	21	19	17	15	24	
9.7	mCherry +	12	20	23	5	15	6	Not integrated
	mCherry -	36	17	12	29	18	24	
3.8	mCherry +	17	4	26	20	22	23	Integrated on Chr. II
	mCherry -	13	23	9	13	8	8	
11.16	mCherry +				14	22	0	Integrated on Chr. X
	mCherry -				6	9	30	
10.12	mCherry +	22	24	5	29	32	11	Not integrated
	mCherry -	9	7	2	2	2	22	
11.6	mCherry +	16	20	14	35	1	32	Integrated on Chr. V
	mCherry -	8	14	10	2	28	1	

The table shows the correlation of visible recessive phenotypes present on the six worm chromosomes I-V and X, and putative integrants of an array containing mCherry. For example, among worms from an individual on master plate 4.16, among 30 worms with the recessive ‘Dumpy’ phenotype due to mutation on chromosome V, only one expressed mCherry, demonstrating anticorrelation of these traits and providing strong evidence that the extrachromosomal array has integrated on chromosome V. Consistent with this interpretation, no other visible marker was anticorrelated with mCherry expression in offspring from this individual.

Table 3. Characterization of putative *cre*-dependent *gfp* integrants crossed with N2 wts

cre-dependent <i>gfp</i> Plate #	# Transgenic Males (%)	# Transgenic Hermaphrodites (%)	Interpretation
*5.14	32 (52.5%)	29 (47.5%)	Putative Autosome Integrant
5.18	33 (89.2%)	4 (10.8%)	Putative Non-Integrant
6.12	34 (77.3%)	10 (22.7%)	Putative Non-Integrant
*6.17	0 (0%)	46 (100%)	Putative Sex Chromosome Integrant
*8.2	46 (61.3%)	29 (38.7%)	Putative Autosome Integrant
*10.19	38 (61.3%)	24 (38.7%)	Putative Autosome Integrant

Putative homozygous integrants (POs) were crossed with wild-type N2 males. Transgenic male progeny of this cross (F1s) were then selected and crossed with wild-type N2 hermaphrodites. mCherry-positive progenies from each of the six F1 crosses were picked and scored for percent males and percent hermaphrodites. Results are shown in the above table. 100% of mCherry-positive progeny being hermaphrodites indicates a likely integration on the X chromosome. Approximately 50% transgenic progenies being male and 50% hermaphrodites indicates a likely integration on an autosome. Transgenic progeny that are significantly more male than hermaphrodites likely indicates a stable array that has not integrated on a chromosome.

* connotes putative integrants selected for confirmatory mapping by crossing with strains EG1000 and EG1020.

Table 4. Identification and mapping of *cre*-dependent *gfp* integrants

Master Plate #		Mapping Strain EG1000			Mapping Strain EG1020			Interpretation
		Dumpy (chr. I)	Roll (chr. II)	Long (chr. III)	Blister (chr. IV)	Dumpy (chr. V)	Long (chr. X)	
8.2	mCherry +	27	28	11	0	23	22	Integrated on Chr. IV
	mCherry -	6	15	6	22	9	5	
6.17	mCherry +				3	25	0	Integrated on Chr. X
	mCherry -				0	7	23	
10.19	mCherry +	6	4	7	22	23	22	Not integrated
	mCherry -	24	12	24	7	8	8	
5.14	mCherry +	24	0	14	20	23	19	Integrated on Chr. II
	mCherry -	6	30	1	7	7	8	

The table shows the correlation of visible recessive phenotypes present on the six worm chromosomes I-V and X. For example, among worms from an individual on master plate 8.2, among 22 worms with the recessive 'blister' phenotype due to mutation on chromosome IV, zero expressed mCherry, demonstrating anticorrelation of these traits and providing strong evidence that the extrachromosomal array has integrated on chromosome IV. Consistent with this interpretation, no other visible marker was anticorrelated with mCherry expression in offspring from this individual.

References

1. Cowan WM, Fawcett JW, O'Leary DD, Stanfield BB. Regressive events in neurogenesis. *Science* 1984;225:1258-65.
2. Duke RC, Cohen JJ. IL-2 addiction: withdrawal of growth factor activates a suicide program in dependent T cells. *Lymphokine Res* 1986;5:289-99.
3. Ellis HM, Horvitz HR. Genetic control of programmed cell death in the nematode *C. elegans*. *Cell* 1986;44:817-29.
4. Ellis RE, Yuan JY, Horvitz HR. Mechanisms and functions of cell death. *Annu Rev Cell Biol* 1991;7:663-98.
5. Jacobson MD, Weil M, Raff MC. Programmed cell death in animal development. *Cell* 1997;88:347-54.
6. Oppenheim RW. Cell death during development of the nervous system. *Annu Rev Neurosci* 1991;14:453-501.
7. Saunders JW, Jr. Death in embryonic systems. *Science* 1966;154:604-12.
8. Mangahas PM, Zhou Z. Clearance of apoptotic cells in *Caenorhabditis elegans*. *Semin Cell Dev Biol* 2005;16:295-306.
9. Peden E, Kimberly E, Gengyo-Ando K, Mitani S, Xue D. Control of sex-specific apoptosis in *C. elegans* by the BarH homeodomain protein CEH-30 and the transcriptional repressor UNC-37/Groucho. *Genes Dev* 2007;21:3195-207.
10. Steller H. Mechanisms and genes of cellular suicide. *Science* 1995;267:1445-9.
11. Sulston JE, White JG. Regulation and cell autonomy during postembryonic development of *Caenorhabditis elegans*. *Dev Biol* 1980;78:577-97.
12. Horvitz HR. Genetic control of programmed cell death in the nematode *Caenorhabditis elegans*. *Cancer Res* 1999;59:1701s-6s.
13. Hedgecock EM, Sulston JE, Thomson JN. Mutations affecting programmed cell deaths in the nematode *Caenorhabditis elegans*. *Science* 1983;220:1277-9.
14. Conradt B, Xue D. Programmed cell death. *WormBook* 2005:1-13.
15. Conradt B, Horvitz HR. The *C. elegans* protein EGL-1 is required for programmed cell death and interacts with the Bcl-2-like protein CED-9. *Cell* 1998;93:519-29.
16. Hengartner MO, Ellis RE, Horvitz HR. *Caenorhabditis elegans* gene *ced-9* protects cells from programmed cell death. *Nature* 1992;356:494-9.
17. Parrish J, Li L, Klotz K, Ledwich D, Wang X, Xue D. Mitochondrial endonuclease G is important for apoptosis in *C. elegans*. *Nature* 2001;412:90-4.
18. Parrish JZ, Xue D. Functional genomic analysis of apoptotic DNA degradation in *C. elegans*. *Mol Cell* 2003;11:987-96.
19. Wang X, Yang C, Chai J, Shi Y, Xue D. Mechanisms of AIF-mediated apoptotic DNA degradation in *Caenorhabditis elegans*. *Science* 2002;298:1587-92.
20. Wu YC, Stanfield GM, Horvitz HR. NUC-1, a *Caenorhabditis elegans* DNase II homolog, functions in an intermediate step of DNA degradation during apoptosis. *Genes Dev* 2000;14:536-48.

21. Chung S, Gumienny TL, Hengartner MO, Driscoll M. A common set of engulfment genes mediates removal of both apoptotic and necrotic cell corpses in *C. elegans*. *Nat Cell Biol* 2000;2:931-7.
22. Ellis RE, Jacobson DM, Horvitz HR. Genes required for the engulfment of cell corpses during programmed cell death in *Caenorhabditis elegans*. *Genetics* 1991;129:79-94.
23. Gumienny TL, Brugnera E, Tosello-Tramont AC, et al. CED-12/ELMO, a novel member of the CrkII/Dock180/Rac pathway, is required for phagocytosis and cell migration. *Cell* 2001;107:27-41.
24. Wang X, Wu YC, Fadok VA, et al. Cell corpse engulfment mediated by *C. elegans* phosphatidylserine receptor through CED-5 and CED-12. *Science* 2003;302:1563-6.
25. Wu YC, Tsai MC, Cheng LC, Chou CJ, Weng NY. *C. elegans* CED-12 acts in the conserved crkII/DOCK180/Rac pathway to control cell migration and cell corpse engulfment. *Dev Cell* 2001;1:491-502.
26. Zhou Z, Hartwig E, Horvitz HR. CED-1 is a transmembrane receptor that mediates cell corpse engulfment in *C. elegans*. *Cell* 2001;104:43-56.
27. McCarthy JV, Dixit VM. Apoptosis induced by *Drosophila* reaper and grim in a human system. Attenuation by inhibitor of apoptosis proteins (cIAPs). *J Biol Chem* 1998;273:24009-15.
28. Reddien PW, Horvitz HR. CED-2/CrkII and CED-10/Rac control phagocytosis and cell migration in *Caenorhabditis elegans*. *Nat Cell Biol* 2000;2:131-6.
29. Wu YC, Horvitz HR. The *C. elegans* cell corpse engulfment gene *ced-7* encodes a protein similar to ABC transporters. *Cell* 1998;93:951-60.
30. Sulston JE, Horvitz HR. Post-embryonic cell lineages of the nematode, *Caenorhabditis elegans*. *Dev Biol* 1977;56:110-56.
31. Horvitz HR. Worms, life, and death (Nobel lecture). *Chembiochem* 2003;4:697-711.
32. Conradt B, Horvitz HR. The TRA-1A sex determination protein of *C. elegans* regulates sexually dimorphic cell deaths by repressing the *egl-1* cell death activator gene. *Cell* 1999;98:317-27.
33. Trent C, Tsuing N, Horvitz HR. Egg-laying defective mutants of the nematode *Caenorhabditis elegans*. *Genetics* 1983;104:619-47.
34. Ellis RE, Horvitz HR. Two *C. elegans* genes control the programmed deaths of specific cells in the pharynx. *Development* 1991;112:591-603.
35. Liu H, Strauss TJ, Potts MB, Cameron S. Direct regulation of *egl-1* and of programmed cell death by the Hox protein MAB-5 and by CEH-20, a *C. elegans* homolog of Pbx1. *Development* 2006;133:641-50.
36. Cao J, Packer JS, Ramani V, et al. Comprehensive single-cell transcriptional profiling of a multicellular organism. *Science* 2017;357:661-7.
37. Avery L, Horvitz HR. A cell that dies during wild-type *C. elegans* development can function as a neuron in a *ced-3* mutant. *Cell* 1987;51:1071-8.
38. Chung K, Crane MM, Lu H. Automated on-chip rapid microscopy, phenotyping and sorting of *C. elegans*. *Nat Methods* 2008;5:637-43.
39. Yandell MD, Edgar LG, Wood WB. Trimethylpsoralen induces small deletion mutations in *Caenorhabditis elegans*. *Proc Natl Acad Sci U S A* 1994;91:1381-5.

40. Thellmann M, Hatzold J, Conradt B. The Snail-like CES-1 protein of *C. elegans* can block the expression of the BH3-only cell-death activator gene *egl-1* by antagonizing the function of bHLH proteins. *Development* 2003;130:4057-71.
41. Brenner S. The genetics of *Caenorhabditis elegans*. *Genetics* 1974;77:71-94.
42. Rhoads A, Au KF. PacBio Sequencing and Its Applications. *Genomics Proteomics Bioinformatics* 2015;13:278-89.
43. See P, Lum J, Chen J, Ginhoux F. A Single-Cell Sequencing Guide for Immunologists. *Front Immunol* 2018;9:2425.
44. Kono N, Arakawa K. Nanopore sequencing: Review of potential applications in functional genomics. *Dev Growth Differ* 2019;61:316-26.
45. Suzanne M, Steller H. Shaping organisms with apoptosis. *Cell Death Differ* 2013;20:669-75.
46. Kirkin V, Joos S, Zornig M. The role of Bcl-2 family members in tumorigenesis. *Biochim Biophys Acta* 2004;1644:229-49.
47. Sulston JE, Schierenberg E, White JG, Thomson JN. The embryonic cell lineage of the nematode *Caenorhabditis elegans*. *Dev Biol* 1983;100:64-119.